doi.org/10.36721/PJPS.2026.39.12.360.1

LncRNA PVT1 in bone marrow mesenchymal stem cells suppresses prostate cancer progression via targeting miR-122 in tumor microenvironment

Jun Liu[1*], Xiaolei Xue[2] and Aikepar·Abulajiang[1]
[1]Department of Urology, Second Affiliated Hospital of Xinjiang Medical Univesity, Urumqi, Xinjiang, 830063, China
[2]Department of Obstetrics, The Fifth Affiliated Hospital of Xinjiang Medical University, Urumqi, Xinjiang, 830000, China

Abstract: **Background**: Prostate cancer progression is influenced by the tumor microenvironment. Bone marrow mesenchymal stem cells (BMSCs) can modulate tumor behavior, but the role of their lncRNA PVT1 is unclear. **Objective**: To investigate whether lncRNA PVT1 in BMSCs regulates the malignant phenotype of prostate cancer cells through miR-122 and elucidate its mechanism of action in the tumor microenvironment. **Method**: Rat BMSCs were isolated and cultured and a Transwell co-culture system was established with human prostate cancer cell lines (PC-3). RT-qPCR was used to detect the expression of PVT1 and miR-122 in BMSCs and cancer cells. PVT1 was overexpressed and knocked down in BMSCs to observe its effects on cancer cell proliferation (CCK-8), apoptosis (flow cytometry) and cell cycle (PI staining) in the co-culture system. The targeting relationship between PVT1 and miR-122 was validated using a dual-luciferase reporter assay. Rescue experiments were performed by simultaneously manipulating PVT1 and miR-122 in BMSCs. **Results**: In prostate cancer patient tissues and cell lines, PVT1 expression was downregulated while miR-122 expression was upregulated. In the co-culture system, overexpression of PVT1 in BMSCs significantly inhibited cancer cell proliferation, arrested the cell cycle at the G0/G1 phase and promoted apoptosis. Conversely, knockdown of PVT1 in BMSCs promoted the malignant phenotype of cancer cells. Mechanistically, PVT1 directly targeted and negatively regulated miR-122. Overexpression of miR-122 reversed the inhibitory effect of PVT1 overexpression in BMSCs on cancer cells. **Conclusion**: BMSCs exert a tumor-suppressive effect in the prostate cancer microenvironment through the PVT1/miR-122 axis, which may serve as a novel therapeutic target for prostate cancer.

Keywords: Bone marrow mesenchymal stem cells; LncRNA PVT1; miR-122; Prostate cancer; Tumor microenvironment

Submitted on 09-12-2025 – Revised on 22-01-2026 – Accepted on 04-02-2026 – Available online on 08-09-2026 – Published on 01-12-2026

INTRODUCTION

Prostate cancer is the second most common cancer worldwide and exhibits a high incidence in China, posing a significant public health burden (Vaccarella *et al*., 2024). Although progress has been made in understanding its molecular mechanisms, the specific pathogenesis remains incompletely elucidated (Pernigoni *et al*., 2023) highlighting the urgent need to identify new therapeutic targets and intervention strategies. Developing effective intervention targets and methods to improve prognosis remains a crucial current direction (Tagawa *et al*., 2024). In this context, non-coding RNAs, particularly long non-coding RNAs (lncRNAs) have emerged as key regulatory factors in tumor biology (Han *et al*., 2022; Eptaminitaki *et al*., 2022). LncRNAs can not only regulate gene expression at the transcriptional and post-transcriptional levels but also participate in complex competing endogenous RNA networks by sponging microRNAs, thereby relieving miRNA-mediated inhibition of target genes, including oncogenes or tumor suppressor genes (Zhao *et al*., 2021; Pronina *et al*., 2023; Shetty *et al*., 2022). This lncRNA-miRNA interaction plays a critical role in tumor progression, metastasis and treatment response (Entezari *et al*., 2022; Wen *et al*., 2023).

Notably, the lncRNA PVT1, located on chromosome 8q24, has been extensively studied in various cancers. However, its functional role appears to be context-dependent. In multiple malignancies, including hepatocellular carcinoma, gastric cancer and cutaneous squamous cell carcinoma, PVT1 has been reported as an oncogene, promoting cell proliferation, invasion and chemotherapy resistant (Li *et al*., 2023). Paradoxically, emerging evidence also suggests that PVT1 may exert tumor-suppressive functions in certain specific contexts, potentially stemming from cell type-specific interactions or regulation by the tumor microenvironment (Tabury *et al*., 2022; Wang *et al*., 2025). In prostate cancer, although differential expression of PVT1 has been observed (Melone *et al*., 2025), its exact function—particularly within the tumor microenvironment—remains unclear and warrants further investigation.

The tumor microenvironment is increasingly recognized as a key determinant of tumor behavior. Bone marrow-derived mesenchymal stem cells (BMSCs) are a critical component of the tumor stroma, capable of homing to

*Corresponding author: e-mail: LiuJun2010_good@163.com

tumor sites and influencing cancer progression through paracrine signaling and direct cell-cell contact (Baron *et al*., 2023). BMSCs can regulate the expression of various miRNAs, which in turn modulate tumor cell proliferation, apoptosis and metastasis (Wang *et al*., 2025). Moreover, miR-122, a well-characterized pro-oncogenic miRNA in multiple cancers, has been shown to participate in cell cycle regulation and metabolic reprogramming (Janosevic *et al*., 2025; Song *et al*., 2025). Interestingly, bioinformatics analysis predicts potential binding sites between PVT1 and miR-122, suggesting the possible existence of a regulatory axis within the ceRNA network.

Beyond classical oncogenic pathways, recent studies emphasize the role of lncRNAs in regulating non-apoptotic cell death programs (such as cuproptosis) and immune checkpoint modulation, offering novel perspectives for prognostic stratification and targeted therapy (Li *et al*., 2023; Gong *et al*., 2024). Additionally, lncRNA-mediated cellular stress responses and metabolic alterations further highlight their pleiotropic functions in tumor adaptation (Ma *et al*., 2024; Chu *et al*., 2022).

Given the reported dual role of PVT1, its potential interaction with miR-122 and the significant influence of BMSCs within the prostate cancer microenvironment, this study hypothesized that BMSC-derived PVT1 may exert tumor-suppressive effects by sponging miR-122, thereby attenuating its pro-oncogenic activity. This study aims to elucidate the expression patterns of PVT1 and miR-122 in prostate cancer tissues and cell lines and to explore the translational potential of the PVT1/miR-122 axis as a therapeutic target. It is hoped that this research will provide new insights into the microenvironmental regulation of prostate cancer and offer perspectives for the development of lncRNA-based intervention strategies.

MATERIALS AND METHODS

The principle of experimental design

All *in-vitro* cytological experiments are designed to include three independent biological replicates, that is, the cells are derived from three separate isolation, passage or cryopreservation batches. At least three technical replicates (such as the triple wells of RT-qPCR, the triple wells of CCK-8 experiment, etc.) are set at the experimental sites within each biological repeat. Strict negative controls (NC) were set up for all function acquisition and function loss experiments.

Cell culture

The human prostate cancer cell line PC-3 was purchased from the American Type Culture Collection (ATCC, USA). The cells were cultured in RPMI-1640 medium (Gibco, USA) supplemented with 10% fetal bovine serum (FBS, Gibco, USA) and maintained under standard conditions in a humidified incubator at 37ºC with 5% CO_2.

Isolation and identification of rat BMSCs

Healthy 4-week-old male Sprague-Dawley rats (SD rats, purchased from the Animal Center of China Three Gorges University) were euthanized by cervical dislocation. Under aseptic conditions in a laminar flow hood, bilateral femurs were isolated. Bone marrow cavity contents were flushed out using low-glucose DMEM medium (Gibco, USA) supplemented with 10% FBS, gently pipetted and seeded into culture dishes. Cells were cultured in complete DMEM/F12 medium (Gibco, USA) containing 10% FBS at 37ºC with 5% CO_2. After 48 h, the medium was completely replaced to remove non-adherent cells and subsequently changed every 3 days. When cells reached 80-90% confluence, they were digested with 0.25% trypsin (containing EDTA) and passaged. Third-passage cells were used for subsequent experiments. BMSCs were identified by flow cytometry (FACSCalibur, BD Biosciences, USA) using surface markers: PE-labeled anti-CD29 and FITC-labeled anti-CD90 antibodies (both from BioLegend, USA) were used to detect positive markers; corresponding antibodies were used to detect the hematopoietic markers CD34 and CD45 (negative markers). Cells meeting the criteria of $CD29^+$, $CD90^+$ (positive rate > 95%), $CD34^-$ and $CD45^-$ were identified as BMSCs. The purity of BMSCs used in this study was 99.2%.

Specimen collection

A total of 25 pairs of prostate cancer tissue samples (cancer tissue and matched adjacent normal tissue) were collected from patients who underwent surgical resection at Second Affiliated Hospital of Xinjiang Medical University. Among them, 13 cases were at stage I+II and 12 cases were at stage III+IV. None of the patients had received any radiotherapy or chemotherapy. After collection, the tissues were immediately snap-frozen in liquid nitrogen and then transferred to a -80ºC freezer for storage.

Basis for sample size calculation: During the experimental design phase, reference was made to the sample size range commonly used in previous exploratory biomarker studies (typically 15–30 pairs) as well as the statistical requirements for preliminary detection of expression differences. Through pre-experimental analysis and literature review (He *et al*., 2018), the significance level (α) was set at 0.05, the statistical power (1-β) was set at 0.80 and the expected effect size (Cohen's d) was set at 1.0. Using G*Power 3.1 software for estimation, the minimum required sample size per group was calculated to be approximately 10–12 cases. To ensure the reliability of comparisons between subgroups (stage I+II vs. stage III+IV), the total sample size was ultimately set at 25 pairs (matched cancer and adjacent tissue samples), comprising 13 cases of stage I+II and 12 cases of stage III+IV. This sample size meets the aforementioned statistical requirements and retains a certain margin for contingencies. It should be noted that this study is exploratory in nature, with the primary aim of providing clinical correlation

evidence to inform subsequent cellular and animal experiments, rather than serving as a definitive diagnostic or prognostic validation. Larger-scale, multi-center clinical cohort validation will be conducted in future work.

Cell transfection

Transfection of BMSCs: BMSCs in the logarithmic growth phase were seeded into 6-well plates at an appropriate density. When cell confluence reached 60-70%, transfection was performed. Using Lipofectamine 3000 transfection reagent (Invitrogen, USA) according to the manufacturer's instructions, PVT1 overexpression plasmid (pcDNA3.1-PVT1), PVT1-specific small interfering RNA (si-PVT1) and their corresponding negative controls (pcDNA3.1-NC, si-NC) were transfected into BMSCs, respectively. Twenty-four hours after transfection, transfection efficiency was verified as follows:(1) For the overexpression group: RT-qPCR was performed to detect the mRNA expression level of PVT1 in BMSCs, confirming a significant upregulation (typically >10-fold) compared to the negative control group. (2) For the knockdown group: Effective downregulation of PVT1 expression (knockdown efficiency >70%) was confirmed. Only when the transfection efficiency met the above criteria the cells were collected for subsequent experiments or for the preparation of conditioned medium.

Transfection of prostate cancer cells: PC-3 cells were transfected using Lipofectamine 3000 transfection reagent (Invitrogen, USA) with miR-122 mimic, miR-122 inhibitor and their respective negative controls (mimic-NC, inhibitor-NC). Twenty-four hours after transfection, RT-qPCR was performed to verify the overexpression or inhibition efficiency of miR-122. The overexpression group (mimic) typically showed a >50-fold upregulation, while the inhibition group (inhibitor) demonstrated a suppression rate >60%, ensuring the validity of subsequent functional experiments.

Co-culture of BMSCs and prostate cancer cells

A 0.4 μm pore-size Transwell co-culture system (Corning, USA) was employed. BMSCs were seeded in the lower chamber of a 24-well plate at a density of 2×10^4 cells/well. PC-3 cells were seeded in the Transwell upper chamber at a density of 1×10^4 cells/well. The co-culture medium consisted of RPMI-1640 supplemented with 10% FBS. The upper chamber was placed into the lower chamber and co-culture was maintained at 37°C with 5% CO_2 for 48–72 hours. After co-culture, PC-3 cells from the upper chamber and BMSCs from the lower chamber were collected separately for subsequent analysis.

Preparation and treatment of BMSCs conditioned medium (CM)

BMSCs were divided into three groups for transfection: The control group (NC-CM, transfected with empty vector), the PVT1 overexpression group (oe-PVT1-CM, transfected with pcDNA3.1-PVT1) and the PVT1 knockdown group (si-PVT1-CM, transfected with si-PVT1). After transfection, cells were cultured for an additional 24 hours. The original medium was discarded and the cells were gently washed twice with PBS, then switched to serum-free DMEM/F12 basal medium for further culture for 48 hours. The cell supernatant was collected, centrifuged at 1200 rpm for 10 minutes at 4°C to remove debris and then filtered through a 0.22 μm pore-size filter for sterilization. The conditioned medium was aliquoted and stored at -80°C. For use, the conditioned medium was mixed with fresh RPMI-1640 medium containing 10% FBS at a 1:1 volume ratio and applied to treat PC-3 cells.

Detection of cell proliferation capacity

PC-3 cells in the logarithmic growth phase were seeded in 96-well plates at a density of 3×10^3 cells per well and subjected to corresponding treatments (e.g., co-culture with differently treated BMSCs or treatment with different conditioned media). At 24, 48 and 72 hours of culture, 10 μL of CCK-8 solution (Dojindo, Japan) was added to each well, followed by further incubation in the incubator for 2 hours. The absorbance (OD) of each well was measured at 450 nm using a microplate reader (BioTek, USA). Cell proliferation curves were plotted with time on the horizontal axis and OD450 values on the vertical axis.

Detection of apoptosis

After harvesting the treated PC-3 cells, they were washed twice with pre-chilled PBS. Staining was performed using the Annexin V-FITC/PI Apoptosis Detection Kit (BD Biosciences, USA): cells were resuspended in 100 μL of 1× binding buffer, followed by addition of 5 μL Annexin V-FITC and 5 μL PI staining solution. The mixture was incubated for 15 min at room temperature in the dark. Subsequently, 400 μL of 1× binding buffer was added and the samples were immediately subjected to flow cytometry. Analysis was carried out using a flow cytometer (EPICS XL, Beckman Coulter, USA) and the proportions of early apoptotic (Annexin V^+/PI^-) and late apoptotic/necrotic (Annexin V^+/PI^+) cells were calculated with FlowJo software (v10.0).

Cell cycle analysis

After collecting the cells and washing them with PBS, they were fixed overnight at 4°C using pre-cooled 70% ethanol. The fixative was removed by centrifugation, followed by one wash with PBS. The cells were then incubated with PBS solution containing 100 μg/mL RNase A in a 37°C water bath for 30 minutes to eliminate RNA. Subsequently, propidium iodide (PI) was added to a final concentration of 50 μg/mL and the cells were stained in the dark at room temperature for 30 minutes. DNA content was detected using a flow cytometer and the distribution ratios of cells in each phase of the cell cycle (G0/G1, S and G2/M phases) were analyzed with ModFit LT software (Verity Software House, USA).

Cell migration and invasion assays

A 24-well Transwell chamber (8.0 μm pore size, Corning, USA) was used for the assays.

Migration assay: PC-3 cells (2×10^4) were resuspended in 200 μL of serum-free RPMI-1640 medium and seeded into the upper chamber. The lower chamber was filled with 600 μL of complete medium (containing 10% FBS) supplemented with different treatment factors (e.g., BMSCs-CM).

Invasion assay: Based on the migration assay, the upper surface of the Transwell membrane was pre-coated with 50 μL of diluted Matrigel (BD Biosciences, USA; diluted 1:8 with serum-free medium) and allowed to solidify at 37°C for 2 hours. All subsequent steps were the same as for the migration assay.

After incubation at 37°C with 5% CO_2 for 24 hours, non-migrated/non-invaded cells on the inner surface of the membrane were gently removed with a cotton swab. Cells that had migrated or invaded to the lower surface of the membrane were fixed with 4% paraformaldehyde for 15 minutes and stained with 0.1% crystal violet for 20 minutes. Following PBS rinses, five random fields per well were photographed under an inverted microscope (Olympus, Japan) and the number of cells was counted.

RT-qPCR

Total RNA from cells or tissues was extracted using TRIzol reagent (Invitrogen, USA). The RNA concentration and purity (A260/A280 ratio between 1.8 and 2.0) were measured using a NanoDrop 2000 spectrophotometer (Thermo Fisher, USA) and RNA integrity was verified by 1% agarose gel electrophoresis. Reverse transcription was performed using the PrimeScript RT reagent Kit (Takara, Japan). Amplification reactions were carried out on an ABI 7900 real-time quantitative PCR system (Applied Biosystems, USA) using SYBR Premix Ex Taq II (Takara, Japan). In this study, GAPDH was selected as the internal reference gene for lncRNA. To confirm its expression stability under the experimental conditions (including different groups and co-culture treatments), the expression variation of candidate reference genes (GAPDH, β-actin, 18S rRNA) was pre-analyzed using geNorm or NormFinder software.

It was confirmed that GAPDH exhibited the highest stability with an M-value < 0.5, making it suitable for normalization in this study. All primers (sequences are shown in Table 1) were validated for amplification efficiency using the standard curve method, with efficiencies ranging from 90-110% (R^2> 0.99), meeting the quantitative requirements. Each sample was tested in three technical replicates. The reaction program was as follows: initial denaturation at 95°C for 30 seconds, followed by 40 cycles of 95°C for 5 seconds and 60°C for 30 seconds. The relative expression levels of target genes were calculated using the $2^{-\Delta\Delta Ct}$ method. All experiments included no-template controls and water controls.

Reverse transcription with stem-loop specificity was performed using the miRcute Plus miRNA First-Strand cDNA Synthesis Kit (Tiangen, China). Quantitative PCR (qPCR) was carried out using the miRcute Plus miRNA Fluorescence Quantitative Detection Kit, with U6 snRNA serving as the internal reference for miRNA. The stability of U6 across different treatment groups and the primer efficiency were also validated. Data analysis was conducted using the $2^{-\Delta\Delta Ct}$ method.

Dual-luciferase reporter gene assay

Based on bioinformatic predictions (Ghafouri-Fard *et al*., 2021), the 3'UTR sequences of wild-type PVT1 (WT) containing potential miR-122 binding sites and their corresponding mutant versions (MUT, with mutated binding site sequences) were cloned into the pmirGLO reporter vector (Promega, USA), respectively. The constructed reporter plasmids were co-transfected with either miR-122 mimic or mimic-NC into PC-3 cells. Forty-eight hours post-transfection, cells were lysed using the Dual-Luciferase Reporter Assay System Kit (Promega, USA). The firefly luciferase and *Renilla* luciferase activities were measured separately using a GloMax 20/20 luminometer (Promega, USA). *Renilla* luciferase activity served as the internal reference and relative luciferase activity was calculated as the ratio of firefly luciferase activity to *Renilla* luciferase activity.

Statistical analysis

All experiments were independently repeated at least three times. Statistical analysis was performed using SPSS 20.0 software (IBM, USA). The Shapiro-Wilk test was used to assess the normality of the data and Levene's test was used to evaluate the homogeneity of variance. If the data met the assumptions of normality and homogeneity of variance, comparisons between two groups were conducted using an independent samples t-test and comparisons among multiple groups were performed using one-way analysis of variance (ANOVA). If overall differences were statistically significant, post-hoc pairwise comparisons were further conducted using the Least Significant Difference (LSD) method or the Student-Newman-Keuls (SNK) method. If the data did not meet the assumptions of normality or homogeneity of variance, non-parametric tests were employed (Mann-Whitney U test for comparisons between two groups and Kruskal-Wallis H test for comparisons among multiple groups). For scenarios involving multiple experimental groups requiring multiple pairwise comparisons, p-values were adjusted using the Bonferroni correction to control the Type I error rate. All hypothesis tests were two-tailed and a corrected $P < 0.05$ was considered statistically significant. The P-values reported in the results are all corrected values.

RESULTS

Low expression of lncRNA PVT1 in prostate cancer

As revealed by RT-qPCR, lncRNA PVT1 was significantly lowly expressed in prostate cancer tissues (Fig. 1A), with lower expression in advanced stage (III+IV) than early stage (I+II)(Fig. 1B). To investigate the impact of intercellular communication within the tumor microenvironment on PVT1 expression, a non-contact Transwell co-culture system using BMSCs and PC-3 cells was established. RT-qPCR results (Fig. 1C) revealed that, compared with monoculture, the expression level of PVT1 in BMSCs was significantly reduced after 48 hours of co-culture with PC-3 cells (approximately 60% decrease, $P < 0.01$). Similarly, PC-3 cells also exhibited a downregulation trend in PVT1 expression after co-culture with BMSCs (approximately 40% decrease, $P < 0.05$). This finding suggests that the interaction between BMSCs and cancer cells within the tumor microenvironment may jointly lead to the suppression of PVT1 expression. To further clarify whether cancer cells affect BMSCs through secreted factors, BMSCs were treated with conditioned medium (CM) from PC-3 cells for 24 hours.As shown in figure 1D, CM from the two cancer cell lines significantly inhibited PVT1 mRNA expression in BMSCs (PC-3 CM: approximately 55% decrease, $P < 0.01$). This indicates that cancer cells may actively remodel the microenvironment via paracrine signaling to suppress PVT1 expression in BMSCs.

Regulation of malignant behavior of prostate cancer cells by PVT1 in BMSCs

To directly validate the function of PVT1 in BMSCs, BMSCs were transfected with either a PVT1 overexpression plasmid (oe-PVT1-CM) or specific siRNA (si-PVT1-CM) and then co-cultured with PC-3 cells.CCK-8 assay results (Figure 2A) showed that compared to co-culture with control BMSCs (NC-CM), the proliferative capacity of PC-3 cells co-cultured with PVT1-overexpressing BMSCs was significantly inhibited (approximately 45% inhibition at 72 hours, $P < 0.001$). Conversely, co-culture with PVT1-knockdown BMSCs (si-PVT1-CM) significantly promoted PC-3 cell proliferation (approximately 35% promotion at 72 hours, $P < 0.01$). Flow cytometry analysis of apoptosis (Fig. 2B) revealed that the total proportion of early and late apoptotic PC-3 cells co-cultured with PVT1-overexpressing BMSCs increased significantly (from 8.2% in NC-CM to 21.5%, $P < 0.001$). In contrast, PVT1 knockdown reduced the apoptosis rate of PC-3 cells to 4.1% ($P < 0.05$). Cell cycle analysis (Fig. 2C) demonstrated that after co-culture with PVT1-overexpressing BMSCs, the proportion of PC-3 cells arrested in the G0/G1 phase increased significantly (from 56.7-72.3%), while the proportion of S-phase cells decreased (from 28.1-18.5%). Conversely, PVT1-knockdown BMSCs promoted more PC-3 cells to enter the S phase (S-phase proportion increased to 35.6%). Transwell assay results (Figs. 2D-E) indicated that co-culture with PVT1-overexpressing BMSCs or treatment with their conditioned medium (oe-PVT1-CM) significantly inhibited the migration and invasion abilities of PC-3 cells (migrating cell count reduced by approximately 60%, invading cell count reduced by approximately 55%, both $P < 0.001$).

Overexpression of miR-122 reverses the tumor-suppressive function of PVT1 in BMSCs

To understand the expression pattern of miR-122 in prostate cancer, its expression levels in clinical samples and cell lines were first detected using RT-qPCR.As shown in figure 3A, compared to paired adjacent normal tissues, miR-122 expression was significantly upregulated in prostate cancer tissues (approximately 2.8-fold, $P < 0.001$). Additionally, the expression of miR-122 in the PC-3 cell line was also significantly higher than in normal prostate epithelial cells RWPE-1 (approximately 3.5-fold, $P < 0.01$, Fig. 3B). After co-culture with PVT1-overexpressing BMSCs (oe-PVT1-CM), the expression level of miR-122 in PC-3 cells was significantly lower than in the control group (NC-CM) (approximately 52% decrease, $P < 0.01$). Conversely, after co-culture with PVT1-knockdown BMSCs (si-PVT1-CM), the miR-122 level in PC-3 cells was significantly elevated (approximately 85% increase, $P < 0.001$). BMSCs themselves also exhibited a corresponding downregulation of miR-122 expression after transfection with oe-PVT1 (approximately 48% decrease) and upregulation after transfection with si-PVT1 (approximately 90% increase), with trends consistent with those observed in the co-cultured cancer cells (Fig. 3C).

Overexpression of miR-122 significantly inhibited cell apoptosis, with the apoptosis rate reduced by approximately 60% compared to the negative control group (mimic-NC) ($P < 0.001$). Conversely, inhibition of miR-122 increased the apoptosis rate by approximately 1.9-fold ($P < 0.01$) (Fig. 3D). Cell cycle analysis (Figure 3E) showed that overexpression of miR-122 significantly increased the proportion of cells in the S phase (from 29.4-41.7%, $P < 0.01$), suggesting it promoted cell cycle progression. In contrast, inhibition of miR-122 led to a significant increase in the proportion of cells in the G0/G1 phase (from 58.1-70.5%, $P < 0.05$), inducing G1 phase arrest.

lncRNA PVT1 targets miR-122

Bioinformatics suggested that miR-122 might bind to the 3'-UTR region of lncRNA PVT1 (Fig. 4A). The dual-luciferase reporter gene assay was carried out and indicated that miR-122 significantly only inhibited the luciferase activity of lncRNA PVT1 wild-type, indicating that miR-122 might bind to lncRNA PVT1 (Fig. 4B).

Table 1: Primer sequences.

Gene Name	Primer type	Primer sequence (5' → 3')	Amplicon size (bp)
LncRNA PVT1	Forward	GAGCAGCACGTGAAGATGGA	138
	Reverse	AGTGCCTGGTCTGAAGCAGT	
GAPDH	Forward	GGAGCGAGATCCCTCCAAAAT	197
	Reverse	GGCTGTTGTCATACTTCTCATGG	
miR-122	Forward	GCGCGTGGAGTGTGACAATGG	60
	Reverse	AGTGCAGGGTCCGAGGTATT	
U6 snRNA	Forward	CTCGCTTCGGCAGCACA	94
	Reverse	AACGCTTCACGAATTTGCGT	

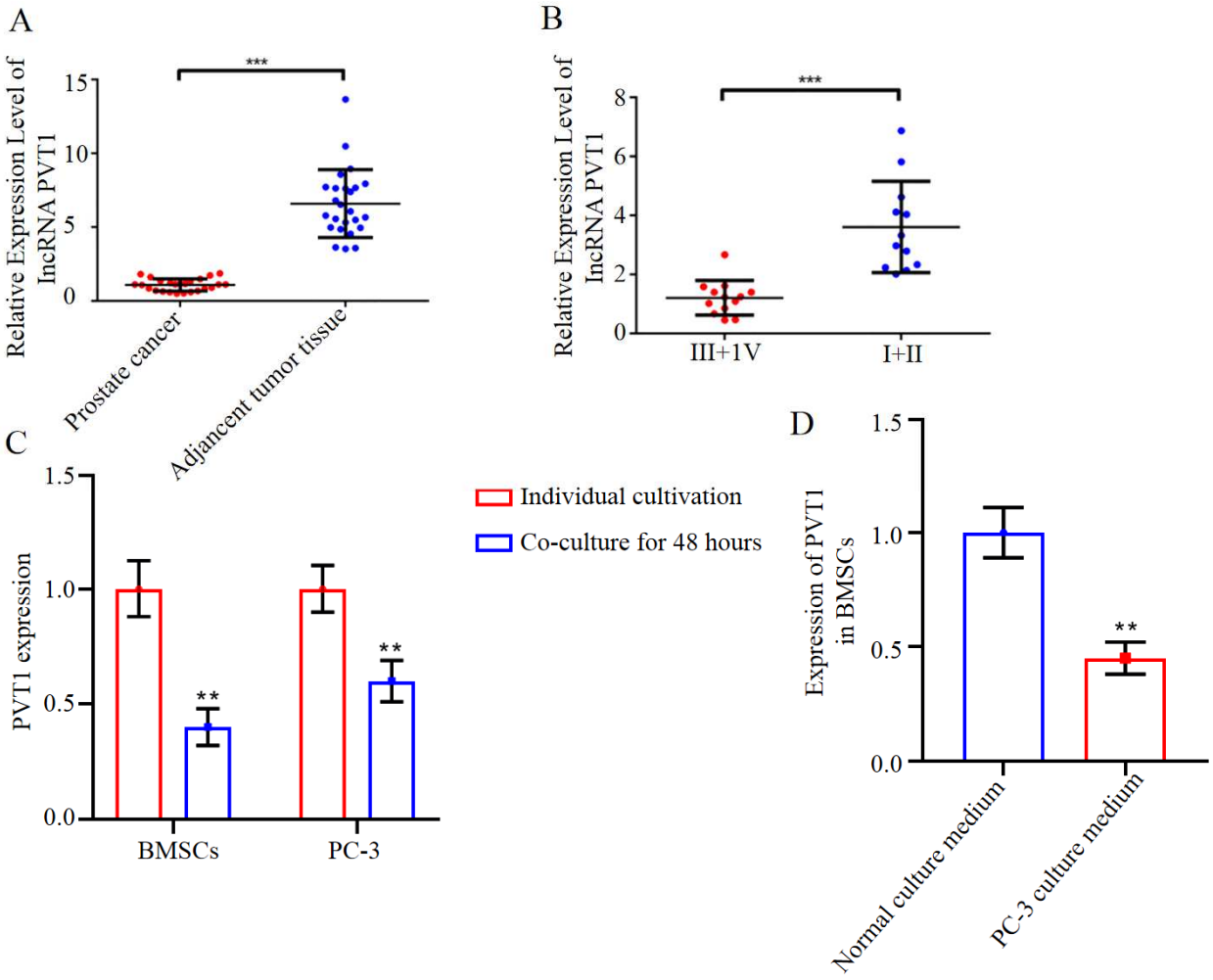

Fig. 1: LncRNA PVT1 is under-expressed in prostate cancer. (A) Expression of PVT1 in prostate cancer tissues and adjacent tissues; (B) Expression of PVT1 in prostate cancer tissues at different stages; (C) Changes in PVT1 expression before and after co-culture of BMSCs with prostate cancer cells; (D) The effect of prostate cancer cell conditioned medium on the expression of PVT1 in BMSC

Overexpression of miR-122 reverses the tumor-suppressive function of PVT1 in BMSCs

To clarify whether miR-122 is a key mediator of PVT1 function, BMSCs were co-transfected with a PVT1 overexpression plasmid (oe-PVT1-CM) and a miR-122 mimic. Compared to the oe-PVT1 group alone, co-transfection with the miR-122 mimic partially reversed the inhibitory effect of PVT1 overexpression on PC-3 cell proliferation (the proliferation rate at 72 hours recovered from 55-78%) (Fig. 5A). Co-transfection with the miR-122 mimic significantly attenuated the increase in PC-3 cell apoptosis induced by PVT1 overexpression (the apoptosis rate decreased from 22.1-12.8%) (Fig. 5B). In migration and invasion experiments, the miR-122 mimic also partially reversed the inhibitory effect of PVT1 overexpression on PC-3 cell motility (Fig. 5C).

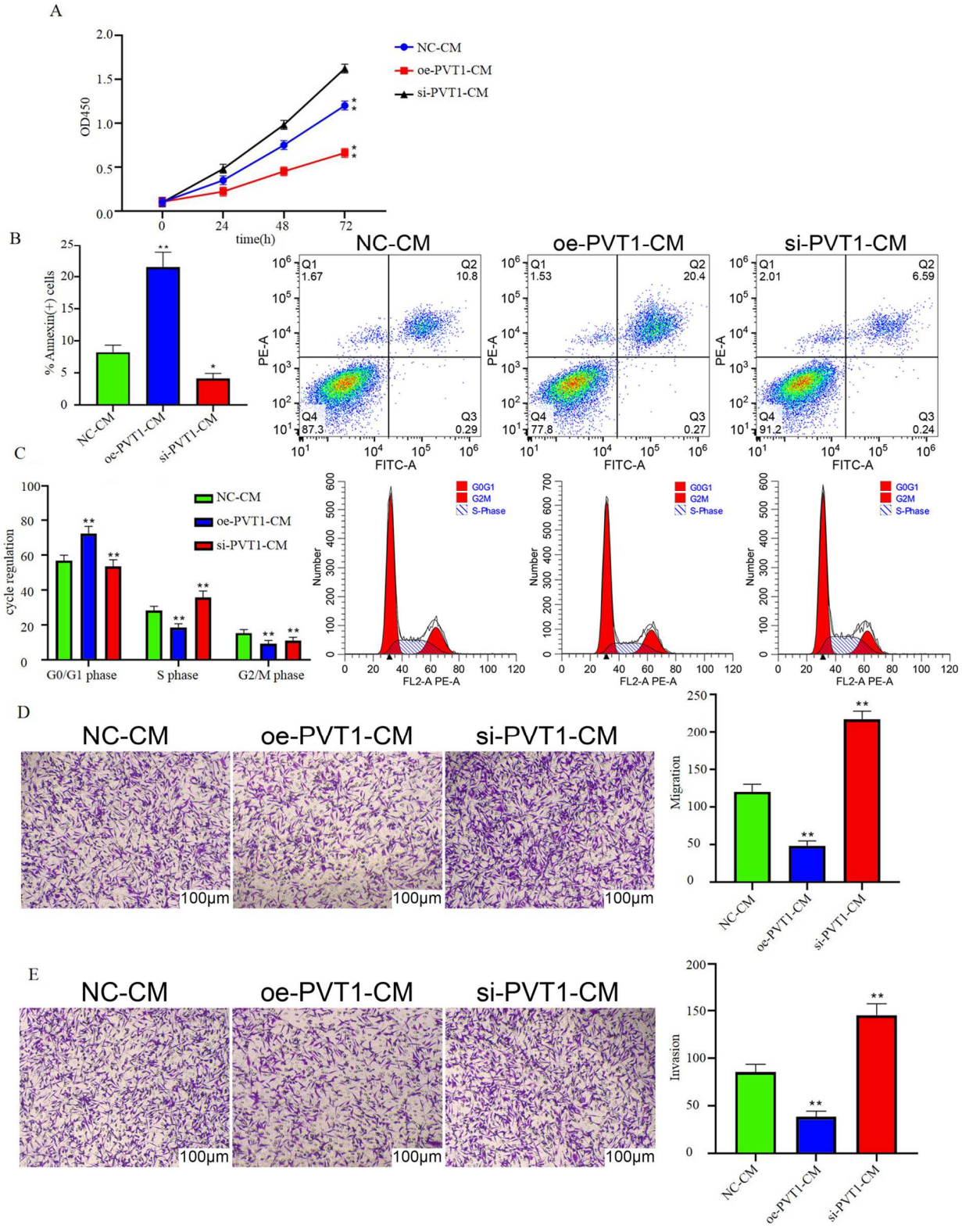

Fig. 2: PVT1 regulates the malignant behavior of prostate cancer cells in BMSCs. (A) CCK-8 was used to detect the effect of overexpression/knockdown of PVT1 in BMSCs on cancer cell proliferation in the co-culture system; (B) Flow cytometry Annexin V/PI detection of the effect of overexpression/knockdown of PVT1 in BMSCs on apoptosis of cancer cells; (C) The effect of overexpression/knockdown of PVT1 in BMSCs on the cycle distribution of cancer cells; (D-E) Transwell assay for the effect of PVT1 in BMSCs on the migration and invasion abilities of cancer cells.

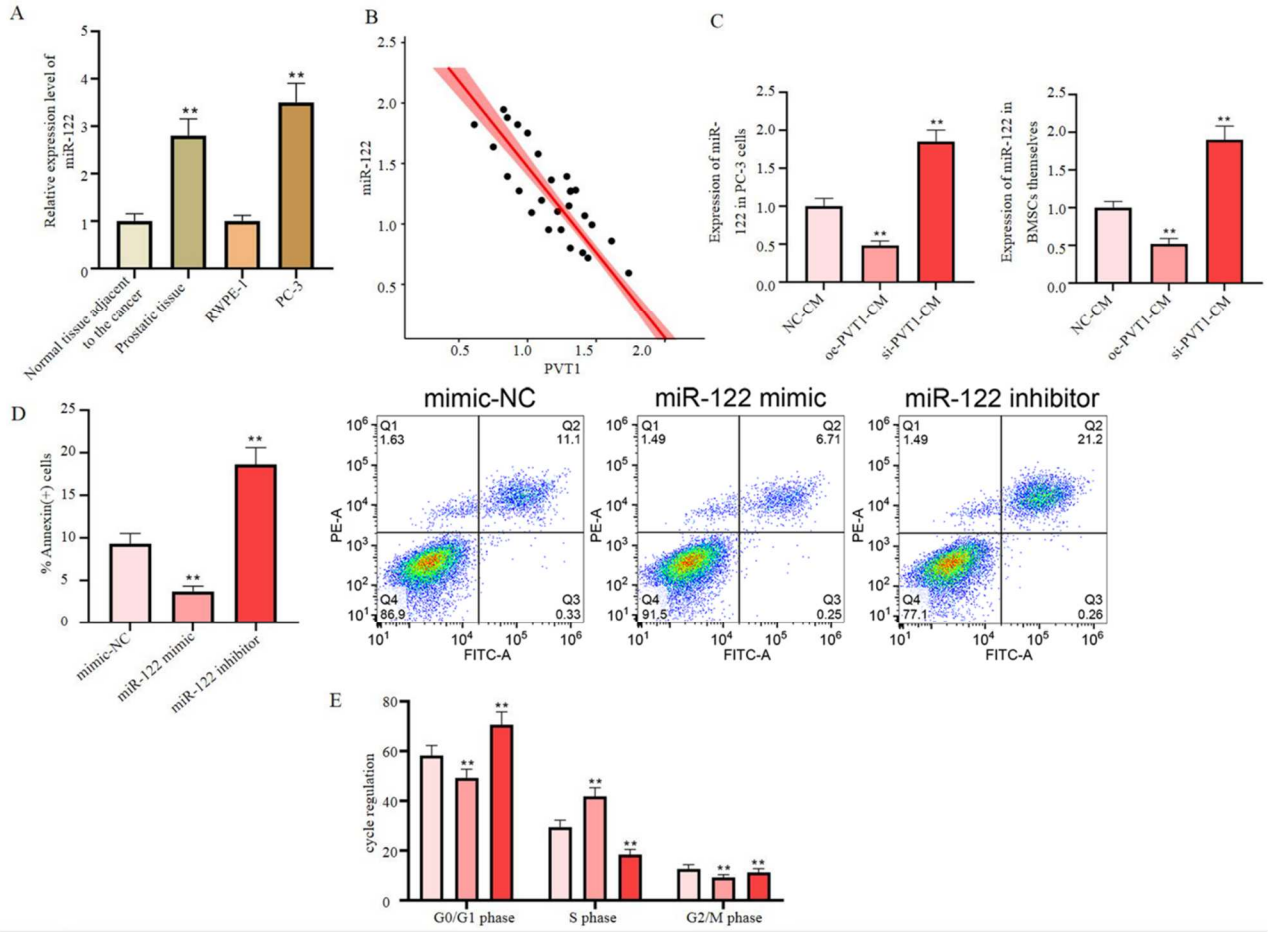

Fig. 3: The role of miR-122 in BMSCS-cancer cell communication. (A-B) The expression of miR-122 in tissues and cells and its correlation with PVT1; (C) The effect of manipulating PVT1 in BMSCs on the expression of miR-122 in co-culture systems. (left) expression of miR-122 in PC-3 cells, (right) expression of miR-122 in PC-3 cells; (D-E) Regulatory effect of miR-122 on apoptosis and cell cycle of cancer cells.

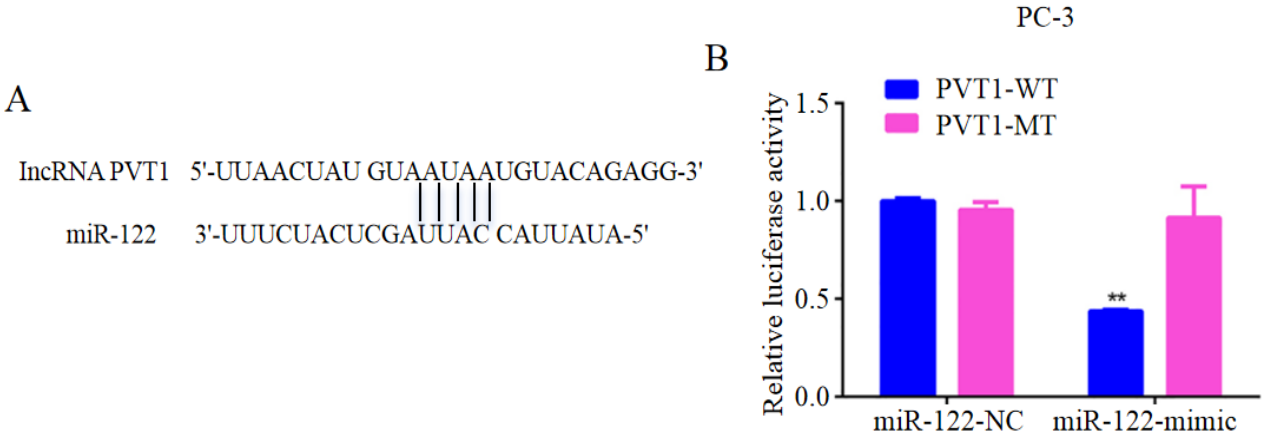

Fig. 4: miR-122 degrades lncRNA PVT1.
(A) Bioinformatics analysis of the binding between miR-122 and lncRNA PVT1.
(B) Luciferase reporter gene assay of relative luciferase activity upon transfection.

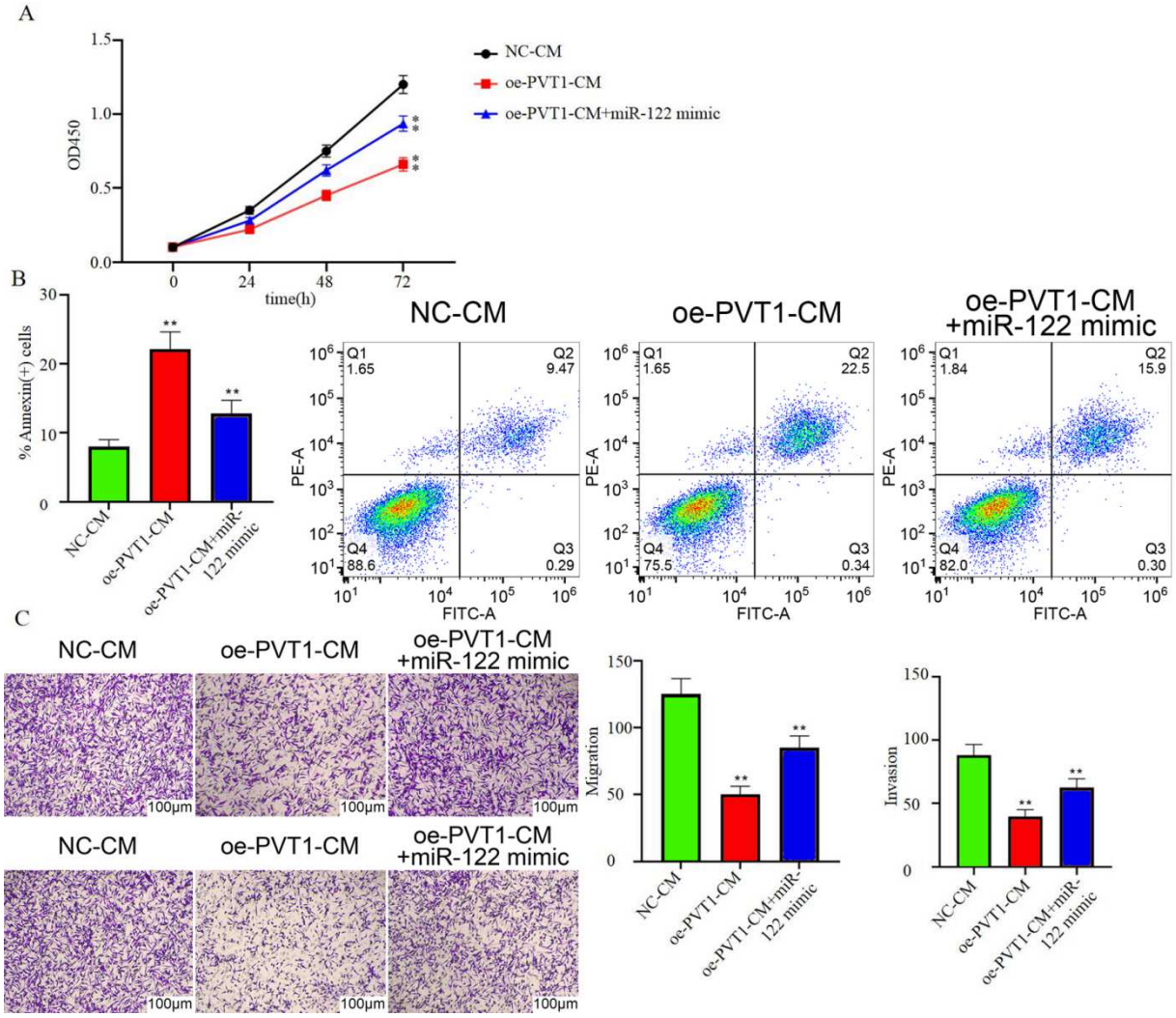

Fig. 5: miR-122 reverses the tumor suppressive function of PVT1 in BMSCs. (A) Cell viability was detected by the CCK-8 method; (B) Apoptosis was detected by Annexin V-FITC/PI double staining flow cytometry. The representative flow chart (left) and quantitative statistics (right) are shown; (C) Transwell assay was used to detect the changes in migration and invasion abilities of PC-3 cells. Representative images of the migration experiment (left image) and invasion experiment (right image, matrix gel spreading room) (top) and cell count statistics (bottom). Scale: 100 μm.

DISCUSSION

This study focuses on stromal–epithelial cell communication within the TME, revealing a novel mechanism by which BMSC-derived lncRNA PVT1 inhibits the malignant phenotype of prostate cancer cells by targeting miR-122. Unlike most studies that concentrate on non-coding RNAs within cancer cells themselves, these findings highlight the crucial role of stromal cells as "senders" of lncRNA signals in regulating tumor progression, offering a fresh perspective for understanding the dynamic complexity of the TME.

These findings first confirm the aberrant expression patterns of PVT1 and miR-122 in prostate cancer at the clinical level. Compared to adjacent normal tissues, the expression of PVT1 was significantly downregulated in prostate cancer tissues, whereas miR-122 expression was markedly upregulated. More importantly, this disparity was more pronounced in patients with advanced-stage (III+IV) disease than in those with early-stage (I+II) disease, suggesting that low PVT1 expression may be associated with disease progression. However, the functions of lncRNAs are highly dependent on their cellular context and interaction networks. Although PVT1 has been reported as an oncogene in various tumors, including colorectal and gastric cancers (Ibrahiem *et al*., 2022; Zeng *et al*., 2021) this study and a few other reports suggest that it may exert tumor-suppressive effects in specific contexts (Nylund *et al*., 2024; Liu *et al*., 2021). This apparent "contradiction" may arise due to tissue or cell type specificity, leading to potential differences in PVT1's expression regulation and

functional partners across different tissues (Ma *et al*., 2025). Additionally, the tumor microenvironment (TME) exerts a certain regulatory influence. In the co-culture experiments of this study, it was observed that cancer cells can actively suppress PVT1 expression in BMSCs through paracrine signaling. This provides a dynamic, cancer cell-driven explanation for the downregulation of PVT1 at the tumor site. Moreover, as a molecular sponge, PVT1 may adsorb different miRNA repertoires in various cancers, thereby activating distinct downstream pathways (Sun *et al*., 2021). Similarly, within the specific context of the prostate cancer TME, PVT1 may primarily function by antagonizing the pro-oncogenic activity of miR-122. This aligns with the direct targeting relationship validated in the dual-luciferase reporter and rescue experiments.

Furthermore, the upregulation of PVT1 in BMSCs sponges miR-122, thereby relieving its inhibition of unknown tumor-suppressive target genes in PC-3 cells. This leads to cell cycle arrest, increased apoptosis and inhibition of migration and invasion in cancer cells within the co-culture system. This "sponging" effect is central to explaining the observed functional phenotypes. However, the efficiency of signal transmission is crucial. As emphasized in previous studies (Choi *et al*., 2025), optimizing delivery systems can significantly enhance the anti-apoptotic effects of active molecules. Therefore, future exploration of how to enhance or mimic the tumor-suppressive signal transmission mediated by PVT1 in BMSCs may provide a promising direction for intervention strategies.

There are however, several important limitations of this study which must be acknowledged. First, the interspecies model employed (co-culture of human prostate cancer cells with rat-derived BMSCs), although common in stromal co-culture studies, may be subject to potential differences in miRNA–lncRNA binding affinity or regulatory networks between species, which could influence the observed interactions. Despite the general conservation of core sequences, the translational relevance of the findings to the human context requires validation using human-derived BMSCs or *in-vivo* models. Second, while the *in-vitro* co-culture system provides compelling evidence for paracrine regulation, it cannot replicate the full complexity of the TME. In the absence of data from animal xenograft models, claims regarding the clinical relevance of the PVT1/miR-122 axis as a therapeutic target remain speculative. Third, this study focused on a single lncRNA–miRNA pair. Both PVT1 and miR-122 are known to have multiple targets. PVT1 likely influences prostate cancer progression through other miRNAs or direct protein interactions and miR-122 undoubtedly regulates a network of genes in cancer cells. The lack of downstream pathway analysis in this study limits the mechanistic depth of the results. Future work should employ techniques such as transcriptome sequencing, proteomics, or pathway-focused analyses to map the downstream consequences of the PVT1/miR-122 interaction.

CONCLUSION

In summary, this study found that BMSC-derived lncRNA PVT1, through its interaction with miR-122, can inhibit the proliferation and migration of prostate cancer cells and promote their apoptosis in an *in-vitro* co-culture model. These results suggest that the PVT1/miR-122 axis may be involved in the stromal–cancer cell communication within the prostate tumor microenvironment, providing new experimental insights into the progression mechanisms of prostate cancer. However, the conclusions of this study are primarily based on cell co-culture experiments and their clinical relevance and potential as therapeutic targets still require further validation through in vivo studies and human-derived models.

Acknowledgments
This work was supported by the Natural Science Foundation of Xinjiang Uygur Autonomous Region, General Program (No.2024D01C15).

Author's contributions
Jun Liu: Conceptualization, Methodology, Investigation (including isolation and culture of BMSCs, cell transfection, co-culture experiments), Formal analysis (RT-qPCR, CCK-8, flow cytometry), Writing – original draft.
Xiaolei Xue: Resources (clinical specimen collection and processing), Investigation (Transwell migration and invasion assays, dual-luciferase reporter assay) Validation, Data Curation, Visualization.
Aikepar· Abulajiang: Supervision, Project administration, Funding acquisition, Writing – Review and Editing, Final approval of the version to be published.
All authors have read and agreed to the published version of the manuscript.

Funding
This research received no external funding.

Data availability statement
The datasets generated and/or analysed during the current study are available from the corresponding author on reasonable request.

Ethical approval
This study involving human specimens was approved by the Ethics Committee of the Second Affiliated Hospital of Xinjiang Medical University (Approval No. (KY2024052108). All procedures were performed in accordance with the ethical standards of the institutional research committee and with the Declaration of Helsinki. Informed consent was obtained from all individual participants included in the study. Animal experiments were conducted in accordance with the guidelines for the care and use of laboratory animals and were approved by the Animal Ethics Committee of Second Affiliated Hospital of Xinjiang Medical University. This study was

performed in adherence with the ARRIVE guidelines. See supplementary file for the ARRIVE checklist.

Conflict of interest

The authors declare no conflicts of interest.

Supplementary data

https://pjps.pk/uploads/2026/09/SUP1788863178.pdf

REFERENCES

Baron M, Drohat P, Crawfor, B, Hornicek F J, Best T M and Kouroupis D (2023). Mesenchymal stem/stromal cells: Immunomodulatory and bone regeneration potential after tumor excision in osteosarcoma patients. *Bioengineering (Basel).*, **10**(10): 1187.

Chu H, Du C, Yang Y, Feng X, Zhu L, Chen J and Yang F (2022). MC-LR Aggravates liver lipid metabolism disorders in obese mice fed a high-fat diet via PI3K/AKT/mTOR/SREBP1 signaling pathway. *Toxins (Basel).*, **14**(12): 833.

Choi YH, Kim HY, Park JO and Choi E (2025). Enhanced anti-tumor effects of natural killer cell-derived exosomes through doxorubicin delivery to hepatocellular carcinoma cells: Cytotoxicity and apoptosis study. *Int J Mol Sci*., **26**(5): 2234.

Entezari M, Taheriazam A, Orouei S, Fallah S, Sanaei A, Hejazi E S, Kakavand A, Rezaei S, Heidari H, Behroozaghdam M, Daneshi S, Salimimoghadam S, Mirzaei, S, Hashemi M and Samarghandian S (2022). LncRNA-miRNA axis in tumor progression and therapy response: An emphasis on molecular interactions and therapeutic interventions.*Biomed Pharmacother.*,**154**: 113609.

Eptaminitaki G C, Stellas D, Bonavida B and Baritaki S (2022). Long non-coding RNAs (lncRNAs) signaling in cancer chemoresistance: From prediction to druggability. *Drug Resist Updat.*, **65**: 100866.

Ghafouri-Fard S, Abak A, Talebi S F, Shoorei H, Branicki W, Taheri M and Akbari Dilmaghani N (2021). Role of miRNA and lncRNAs in organ fibrosis and aging. *Biomed Pharmacother.*, **143**: 112132.

Gong H, Liu Z, Yuan C, Luo Y, Chen Y, Zhang J, Cui Y, Zeng B, Liu J, Li H and Deng Z (2024). Identification of cuproptosis-related lncRNAs with the significance in prognosis and immunotherapy of oral squamous cell carcinoma. *Comput Biol Med.*, **171**: 108198.

Han X, Mo J, Yang Y, Wang Y and Lu H (2022). Crucial roles of lncRNAs-mediated autophagy in breast cancer. *Int J Med Sci.*, **19**(6):1082–1092.

He JH, Han ZP, Zou MX, Wang L, Lv YB, Zhou JB, Cao MR and Li YG (2018). Analyzing the lncRNA, miRNA and mRNA regulatory network in prostate cancer with bioinformatics software. *J Comput Biol.*, **25**(2): 146–157.

Ibrahiem AT, Makhdoom AK, Alanazi KS, Alanazi AM, Mukhlef AM., Elshafey SH, Toraih EA and Fawzy MS (2022). Analysis of anti-apoptotic PVT1 oncogene and apoptosis-related proteins (p53, Bcl2, PD-1 and PD-L1) expression in thyroid carcinoma. *J Clin Lab Anal.*, **36**(5): e24390.

Janosevic D, De Luca T, Melo Ferreira R, Gisch DL, Cheng YH, Hato T, Luo J, Yang Y, Hodgin JB, Phillips CL, Dagher PC, Kidney Precision Medicine Project and Eadon M T (2025). miRNA and mRNA signatures in human acute kidney injury tissue. *Am J Pathol.*, **195**(1): 102–114.

Li R, Huang D, Ju M, Chen HY, Luan C, Zhang JA and Chen K (2023). The long non-coding RNA PVT1 promotes tumorigenesis of cutaneous squamous cell carcinoma via interaction with 4EBP1. *Cell Death discovery.*, **9**(1): 101.

Li Y, Na F and Pei J (2023). Construction and characterization of a cuproptosis- and immune checkpoint-based LncRNAs signature for breast cancer risk stratification. *Breast cancer .*, **30**(3): 393–411.

Liu W, Yao D and Huang B (2021). LncRNA PVT1 promotes cervical cancer progression by sponging miR-503 to upregulate ARL2 expression. *Open Life Sci.*, **16**(1): 1–13.

Ma W, Xu L, Wang Y, Chen S, Li D, Huo X, Li R, Zhu X, Chen N, Jin Y, Luo J, Li C, Zhao K, Zheng Y, Han W and Yu D (2024). piR-27222 mediates PM2.5-induced lung cancer by resisting cell PANoptosis through the WTAP/m6A axis. *Environ. Int.*, **190**: 108928.

Ma X, Chen J and Zhou C (2025). Circular RNA PVT1 as a potential biomarker for human cancers: A systematic review and meta-analysis. *Int. J. Biol. Markers.*, **40**(3): 158–165.

Melone V, Palumbo D, Palo L, Brusco N, Salvati A, Tarallo A, Giurato G, Rizzo F, Nassa G, Weisz A and Tarallo R (2025). LncRNA PVT1 links estrogen receptor alpha and the polycomb repressive complex 2 in suppression of pro-apoptotic genes in hormone-responsive breast cancer. *Cell Death Dis.*, **16**(1): 80.

Nylund P, Garrido-Zabala B, Parraga AA, Vasquez L, Pyl PT, Harinck GM, Ma A, Jin J, Oberg F, Kalushkova A and Wiklund HJ (2024). *PVT1* interacts with polycomb repressive complex 2 to suppress genomic regions with pro-apoptotic and tumour suppressor functions in multiple myeloma. *Haematologica.*, **109**(2): 567–577.

Pernigoni N, Guo C, Gallagher L, Yuan W, Colucci M, Troiani M, Liu L, Maraccani L, Guccini I, Migliorini D, de Bono J and Alimonti A (2023). The potential role of the microbiota in prostate cancer pathogenesis and treatment. *Nat Rev Urol.*, **20**(12): 706–718.

Pronina IV, Filippova EA, Brovkina OI, Burdennyy AM, Kazubskaya TP, Kushlinskii DN, Zhordania KI, Karpukhin AV, Loginov VI, Braga EA and Kushlinskii NE (2023). Long non-coding RNAs and microRNAs groups in the regulation of expression level of a number of tumor-associated genes in ovarian cancer. *Bull Exp Biol Med.*, **174**(3): 354–359.

Shetty A, Venkatesh T, Kabbekodu SP, Tsutsumi R and

Suresh PS (2022). LncRNA-miRNA-mRNA regulatory axes in endometrial cancer: A comprehensive overview. *Arch Gynecol Obstet.*, **306**(5): 1431–1447.

Song CS, Wang GH, Mao PP, Zhang HS, Liu L, Ma XJ, Li XD and Zhang Y (2025). Hypoxia-induced suppression of FAM99A and FAM99B contributes to the development and glucose metabolic reprogramming of hepatocellular carcinoma. *FASEB J* ., **39**(14): e70869.

Sun Y, Zong C, Liu J, Zeng L, Li Q, Liu Z, Li Y, Zhu J, Li L, Zhang C and Zhang W (2021). C-myc promotes miR-92a-2-5p transcription in rat ovarian granulosa cells after cadmium exposure. *Toxicol Appl Pharmacol.*, **421**: 115536.

Tabury K, Monavarian M, Listik E, Shelton AK, Choi AS, Quintens R, Arend RC, Hempel N, Miller CR, Gyorrfy B and Mythreye K (2022). PVT1 is a stress-responsive lncRNA that drives ovarian cancer metastasis and chemoresistance. *Life Sci Alliance.*, **5**(11): e202201370.

Tagawa ST, Thomas C, Sartor AO, Sun M, Stangl-Kremser J, Bissassar M, Vallabhajosula S, Huicochea Castellanos S, Nauseef JT, Sternberg CN, Molina A, Ballman K, Nanus DM, Osborne JR and Bander NH (2024). Prostate-specific membrane antigen-targeting alpha emitter via antibody delivery for metastatic castration-resistant prostate cancer: A phase i dose-escalation study of 225Ac-J591. *J Clin Oncol.*, **42**(7): 842–851.

Vaccarella S, Li M, Bray F, Kvale R, Serraino D, Lorenzoni V, Auvinen A and Dal Maso L (2024). Prostate cancer incidence and mortality in Europe and implications for screening activities: Population based study. *BMJ.*, **386**: e077738.

Wang D, Li Y, Peng X, Zhang L, Zhang Y, Guan X, Liang X, Fu S and Yu J (2025). Calcium overload via PVT1 reprograms neutrophil fate and constrains gastric cancer progression. *J Transl Med.*, **23**(1): 878.

Wang M, Zheng Y, Hao Q, Mao G, Dai Z, Zhai Z, Lin S, Liang B, Kang H and Ma X (2025). Hypoxic BMSC-derived exosomal miR-210-3p promotes progression of triple-negative breast cancer cells via NFIX-Wnt/β-catenin signaling axis. *J Transl Med.*, **23**(1): 39.

Wen JL, Ruan ZB, Wang F and Hu Y (2023). Progress of circRNA/lncRNA-miRNA-mRNA axis in atrial fibrillation. *PeerJ.*, **11**: e16604.

Zeng L, Yuan S, Zhou P, Gong J, Kong X and Wu M (2021). Circular RNA Pvt1 oncogene (CircPVT1) promotes the progression of papillary thyroid carcinoma by activating the Wnt/β-catenin signaling pathway and modulating the ratio of microRNA-195 (miR-195) to vascular endothelial growth factor A (VEGFA) expression. *Bioengineered.*, **12**(2): 11795–11810.

Zhao X, Yang Y and Yin M (2021). MHRWR: Prediction of lncRNA-disease associations based on multiple heterogeneous networks. *IEEE/ACM Trans Comput Biol Bioinform.*, **18**(6): 2577–2585.